Analysis of a rapid load test on an instrumented bored pile in clay

Brown, Michael; Hyde, A. F. L.; Anderson, W. F.

Published in:
Géotechnique

DOI:
10.1680/geot.2006.56.9.627

Publication date:
2006

Document Version
Publisher's PDF, also known as Version of record

Brown, M. J., Hyde, A. F. L. & Anderson, W. F. (2006). *Géotechnique* **56**, No. 9, 627–638

Analysis of a rapid load test on an instrumented bored pile in clay

M. J. BROWN*, A. F. L. HYDE† and W. F. ANDERSON†

Rapid load testing methods for piled foundations are generally easier and quicker to mobilise than classic static tests, and are less complex to analyse than dynamic load tests. A recently developed rapid load pile testing method known as the Statnamic test is seeing greater use in the UK for the assessment of piles. For foundation design, it is necessary to derive the equivalent static load–settlement curve from the rapid load test data by eliminating inertial and damping effects. Existing methods of test analysis generally provide good correlation with static tests for sands and gravels, but overpredict pile capacities by up to 50% for clays. In order to gain an insight into the behaviour of rapid load pile testing in clays, a full-scale pile instrumented with accelerometers, strain-gauged sister bars and a tip load cell was tested in a glacial lodgement till near Grimsby, UK. The soil around the pile was also instrumented with radially arrayed buried accelerometers. The test pile was subjected to rapid loading tests, the results of which were compared with constant rate of penetration and maintained load static tests on the same pile. Results from the field testing have been analysed using non-linear viscous parameters obtained from laboratory model and element tests to represent rate-dependent clay shear resistance in the post-yield phase of loading. Shaft frictions derived from the strain-gauged reinforcement in the pile have been compared with shear strains and stresses derived from accelerations in the surrounding soil to give an insight into the load transfer mechanisms for a rapidly loaded pile in clay.

KEYWORDS: clays; dynamics; field instrumentation; full-scale tests; glacial soils; piles

Les tests de chargement rapides pour des fondations de pieux offrent généralement des méthodes plus faciles et plus rapidement mobilisables que les tests statiques traditionnels, et ils sont également moins complexes à analyser que les tests de chargement dynamiques. Une méthode de chargement de pieu à courte durée connue sous le nom d'essai statnamique voit son utilisation se développer au Royaume-Uni pour l'évaluation des pieux. Pour la conception des fondations, il est nécessaire de dériver la courbe de charge-tassement des données équivalente des tests de chargement rapides en éliminant les effets d'inertie et d'amortissement. Les méthodes existantes d'analyse des essais fournissent généralement une bonne corrélation avec les tests statiques pour les sables et les graviers, mais surestiment les capacités du pieu jusqu'à 50 % pour les argiles. Afin de mieux comprendre le comportement des tests de chargement de pieu rapides dans les argiles, un pieu instrumenté de pleine échelle, disposant d'accéléromètres, de barres jumelles munies de jauge de déformation et d'une cellule de mesure a été testé dans une moraine de fond glaciaire à Grimsby, au Royaume-Uni. Le terrain autour du pieu était également équipé d'accéléromètres enterrés radialement. Le pieu servant à l'essai a été soumis à des tests de chargement rapides, dont les résultats ont été comparés à ceux obtenus pour des tests de chargement statiques maintenus et avec un taux de pénétration constant sur la même pile. Les résultats de l'expérimentation in situ ont été analysés au moyen de paramètres de viscosité non linéaires obtenus à partir de tests d'éléments et de modèle de laboratoire pour représenter la résistance au cisaillement de l'argile dépendante du taux dans la phase post-élasticité de la charge. Les frottements au fût dérivés du renforcement jaugé en déformation dans le pieu ont été comparés avec les déformations et contraintes de cisaillement dérivées d'accélérations dans le sol environnant pour donner un meilleur aperçu des mécanismes de transfert de charge pour un pieu rapidement chargé dans l'argile.

INTRODUCTION

Traditionally, pile load testing is carried out using static methods, which are relatively simple to undertake and analyse but require substantial temporary infrastructure that increases with pile ultimate load capacity, making them expensive and time consuming.

In recent decades dynamic pile testing methods have been developed that require minimal infrastructure but are complicated to analyse. They may also result in pile damage owing to the generation of tensile stresses as a result of the very short loading period of 5–10 ms. Rapid load test (RLT) methods have been developed as an alternative: they utilise the advantages of both static and dynamic tests while avoiding some of the disadvantages. The commonest rapid load testing method, known as the Statnamic test (Fig. 1), works by the rapid burning of a fuel that produces gas in a pressure chamber (Middendorp, 1993). This gas accelerates a reaction mass upwards at a maximum peak acceleration of about 20*g*, which in turn imparts a downward load on the test pile. Thus only 5% of the reaction mass used during static testing is required to produce the same load (Middendorp, 2000). The maximum load and its duration are regulated by controlling the quantity of fuel and the venting of the gas. The load duration is normally regulated to about 200 ms. This loading period is between 20 and 40 times greater than that for a dynamic test, thus avoiding the generation of tensile stresses for piles of up to 40 m length (Middendorp & Bielefeld, 1995; Nishimura & Matsumoto, 1995; Mullins *et al.,* 2002).

For foundation design, it is necessary to derive an equivalent static load–settlement curve from the rapid load test data by eliminating rate effects. The most common form of

Manuscript received 26 October 2004; revised manuscript accepted 16 August 2006.
Discussion on this paper closes on 1 May 2007, for further details see p. ii.
* Division of Civil Engineering, University of Dundee, UK.
† Department of Civil and Structural Engineering, University of Sheffield, UK.

Fig. 1. 3 MN Statnamic testing device

analysis currently used is the unloading point method or UPM (Kusakabe & Matsumoto, 1995), which takes into account both velocity-dependent soil viscous damping and acceleration-dependent pile inertia. However, this method assumes that the soil viscous damping is linear with velocity. Soil damping in clays is highly non-linear, and forms an important component of ultimate pile resistance at enhanced rates of testing (Hyde *et al.,* 2000; Brown, 2004). The UPM method provides a good correlation with static tests for sands and gravels (Brown, 1994; McVay *et al.*, 2003; Wood, 2003), where viscous damping is negligible, but overpredicts pile capacities by up to 50% for clay soils (Holeyman *et al.*, 2000).

In order to gain a better understanding of the load transfer mechanisms under rapid loading, and to improve the analysis of these types of test in clay soils, a full-scale auger-bored pile, instrumented with strain gauges and accelerometers, was installed in a glacial lodgement till with buried accelerometers. Rapid load test results are compared with those from standardised static load tests.

FIELD PILE STUDY

The Grimsby research site was located in a piling contractor's plant yard near Waltham, Grimsby, UK. The ground conditions at the test site comprised matrix-dominant glacial lodgement till (Weltman & Healy, 1978), which was underlain by Cretaceous chalk bedrock (Powell & Butcher, 2003). The till of this region is described as being stiff to firm, greyish to dark brown, predominantly silty clay with a variety of cobbles, boulders and pebbles (Berridge & Pattison, 1994). It is cohesive, overconsolidated, but may also be soft and weathered (reddish brown) with grey joint surfaces (Bell, 2001).

Ground investigation and laboratory soils testing

Two cable percussive boreholes were undertaken adjacent to the test pile location, which encountered 2·4 m of firm to very stiff slightly gravelly orangey brown clay, followed by 18 m of firm to very stiff gravelly greyish brown to dark brown clay with occasional coarse gravel and rare cobbles. The underlying bedrock was not encountered during the investigation. In the first borehole alternate U100 sampling and standard penetration testing (SPT) was undertaken at approximately 1 m vertical centres, and continuous U100 sampling was carried out in the second borehole to recover samples for laboratory triaxial testing (Balderas-Meca, 2004). Additional in situ testing was undertaken using piezocone penetration testing (PCPT) and surface to downhole seismic CPT (SCPT). The results are shown in Fig. 2. Results for multistage undrained triaxial testing (Anderson, 1974) carried out on 100 mm diameter samples are shown in Fig. 3 together with those from previous undrained testing of 38 mm diameter samples (Taylor, 1966) and on-site hand shear vane tests. Further laboratory test results are summarised in Table 1. The soil profile encountered during in situ and laboratory testing suggests that the upper soil layers had previously been exposed to weathering and desiccation. The observed low CPT readings in the top 1·8 m are not representative of the final site conditions as the surface material was replaced with compacted fill for a piling working platform after the borehole and CPT investigation.

Pile description and installation

The instrumented test pile was a 600 mm nominal diameter bored cast in situ pile installed using a standard flat-bladed rotary clay auger to 12·1 m below ground level (BGL) (Fig. 4). Only simple total stress design calculations were undertaken for selection of the pile dimensions based upon the site investigation data shown in Fig. 3. After boring to a depth of 2 m, a steel friction-reducing casing of 610 mm external diameter and 8 mm wall thickness was inserted to 1·8 m BGL with 480 mm left above ground. This was to act as a sleeve, reducing the influence of the variation in soil properties for the desiccated clay layer and pile rig working platform. After reaching the final depth the unsupported bore was inspected and cleaned out using a barrel-like tool with a blade at its base. A tip load cell was then installed on a bed of cement grout, and an instrumented reinforcing cage, incorporating strain-gauged sister bars and embedded accelerometers, was lowered to just above the tip load cell. The reinforcement consisted of six vertical 12 m long T16 bars with a single T12 helical at 300 mm vertical centres. The reinforcing cage was initially tied together and then spot-welded to minimise flexure of the cage during craneage and thus reduce the risk of instrumentation damage. The pile concrete (C35, 10 mm aggregate), which had a 28-day strength of 36 N/mm^2 and an average density of 2·35 Mg/m^3 was poured within 6 h of excavating the bore.

Pile instrumentation

The sister bars incorporated in the pile consisted of 15 strain-gauged T12 reinforcing bars 1 m in length, three at each of five different levels, tied to the horizontal reinforcement (Fig. 4). The three bars at each level were spaced equally around the pile circumference. The sister bars incorporated bonded foil strain gauges rather than the more commonly employed vibrating wire type, which, though durable, are unsuitable for high-frequency loading (Dunnicliff & Green, 1988). The foil gauges were protected by coating with polyurethane followed by several coats of epoxy resin. Finally, the central 150 mm of sister bar was

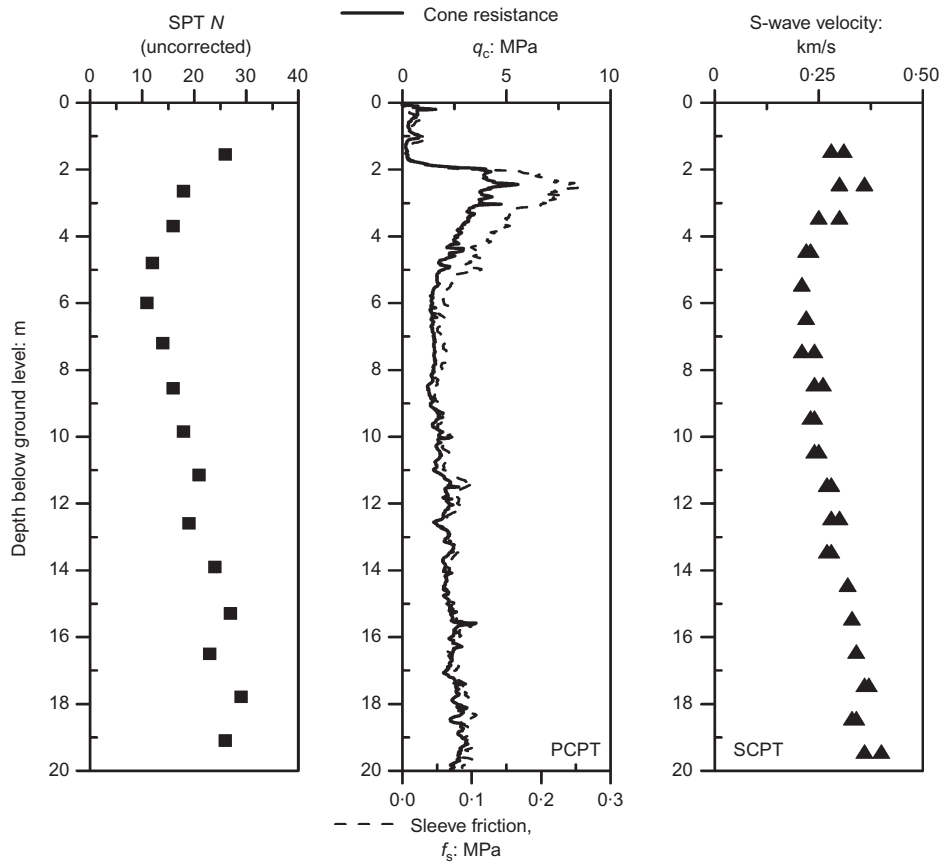

Fig. 2. Results from in situ testing in glacial lodgement till

covered with a protective layer of adhesive-lined shrink-fit plastic. This coating also acted to debond the gauged length from the concrete.

The two piezoelectric shear-type accelerometers embedded in the pile were sealed in waterproof protective stainless steel housings (140 mm in length and 25 mm outer diameter) and secured to the pile reinforcement at two levels. To avoid the unwanted build-up of moisture within the enclosures a chemical desiccant was included with the accelerometers. The accelerometers and protective housings had a low mass to minimise inclusion effects such as frequency alteration.

The pile-tip load cell was also installed to investigate the significant differences between shaft and tip response during rapid load tests as identified by Brown (2004). The pile-tip load cell consisted of an upper and lower plate separated by three strain-gauged load columns (Fig. 5), calibrated in the laboratory to a maximum load of 600 kN. The upper and lower load cell plates were fabricated from 40 mm thick mild steel plate, 500 mm in diameter. Each load column consisted of a cylinder 210 mm in length with an outer diameter of 43·74 mm and a wall thickness of 18·74 mm machined from high-strength, low-hysteresis stainless steel. The strain gauges on the load columns were protected by layers of polyurethane and wax, and then the whole column was surrounded by a thin-walled stainless steel cylinder that slotted into O-ring seals in the top and bottom end plates (Brown, 2004). The cable from the load cell was taken to the surface via two lengths of galvanised steel pipe cast in the pile. This was surrounded by a PVC pipe to de-bond it from the concrete. An inflatable packer was incorporated between the top and bottom plates of the load cell to prevent the concrete from encasing the load cell (Fig. 6). This was inflated with water to the in situ hydrostatic head of 120 kPa prior to the pouring of concrete, and left pressurised for 24 h after concreting.

Soil instrumentation

Six accelerometers in similar housings to those installed in the pile were also installed in the soil surrounding the pile. As shown in Fig. 4 these were installed at two levels (4 m and 8 m BGL) corresponding to the levels of the accelerometers installed in the pile, with three at each level (4 m BGL: 3·05R, 5·04R and 8·5R; 8 m BGL: 2·89R, 4·70R and 9·12R, where R is the pile radius). The radial locations of the accelerometers were chosen based upon accelerations measured in a related laboratory calibration chamber study into the behaviour of model piles subject to rapid loading (Brown, 2004). To install the accelerometers a hollow casing of 36 mm internal diameter with a sacrificial tip was pushed to the required depth. The accelerometer in its own protective casing was lowered down the hollow casing until contact was made with the tip. The casing was then withdrawn as a cement/bentonite grout was poured down the casing.

PILE TEST RESULTS

The pile testing programme was designed to compare the results from rapid and static load tests. Rapid load pile testing commenced 35 days after the pile was installed. The pile was subjected to five different target levels of rapid loading over a two-day period with an initial test taken to 1163 kN on the first day followed by peak loads of 1700, 2048, 2525 and 3071 kN on the second day (Table 2). The actual peak loads measured at the pile head were always higher than the related target loads. This was followed 21 days later by a constant rate of penetration (CRP) test and a further 5 days after this by a maintained load test (MLT). Constant rate of penetration testing was carried out at 0·01 mm/s (ICE, 1997). The maintained load test was undertaken as a proof load test followed by an extended proof load test to the same specification. The design verifica-

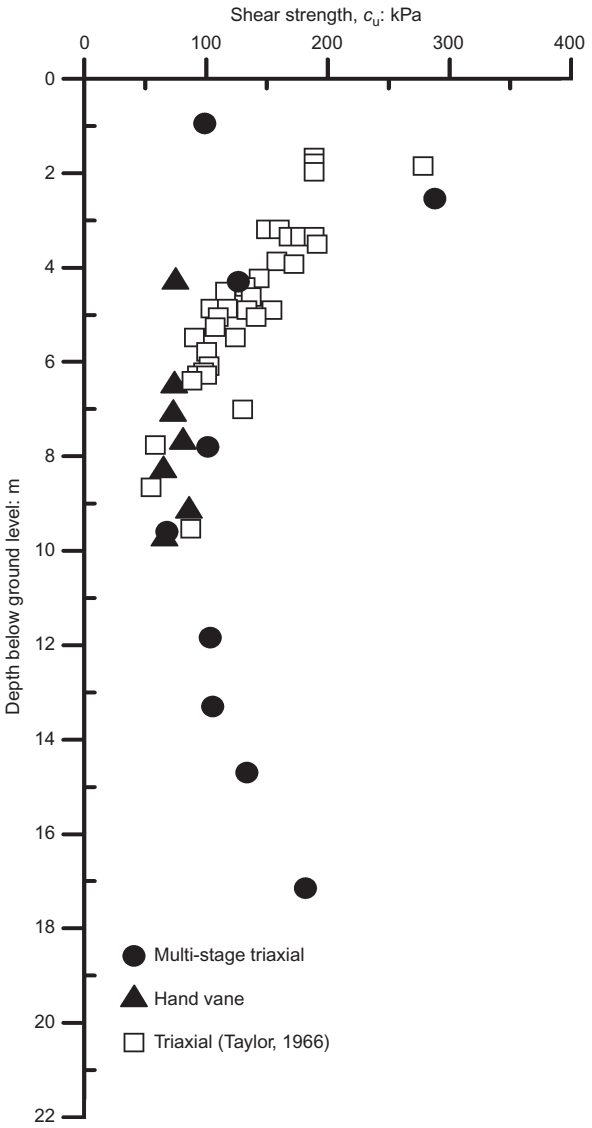

Fig. 3. Shear strength variation with depth for lodgement till

Table 1. Strength and undrained properties for glacial lodgement till

Property	Value
Liquid limit: %	20–36
Plastic limit: %	12–18
Plasticity index: %	7–20
Moisture content: %	14–24
Specific gravity of solids	2.69
Clay fraction: % $< 2\ \mu$m	20–38
Activity	0·35–1·07
Coefficient of vertical permeability at void ratios of 0·40–0·42: m/s	$3–5 \times 10^{-11}$
C_c	0·03–0·04
e_0	0·53–0·64
Slope of critical state line projected to q'–p' plane	1.07

tion load chosen was 900 kN with a specified working load of 900 kN (ICE, 1997). The testing programme is summarised in Table 2, which also lists the exact time intervals between the different tests.

For rapid loading, a 3 MN tripod Statnamic device was used with a hydraulic catch mechanism and 18 t weight pack

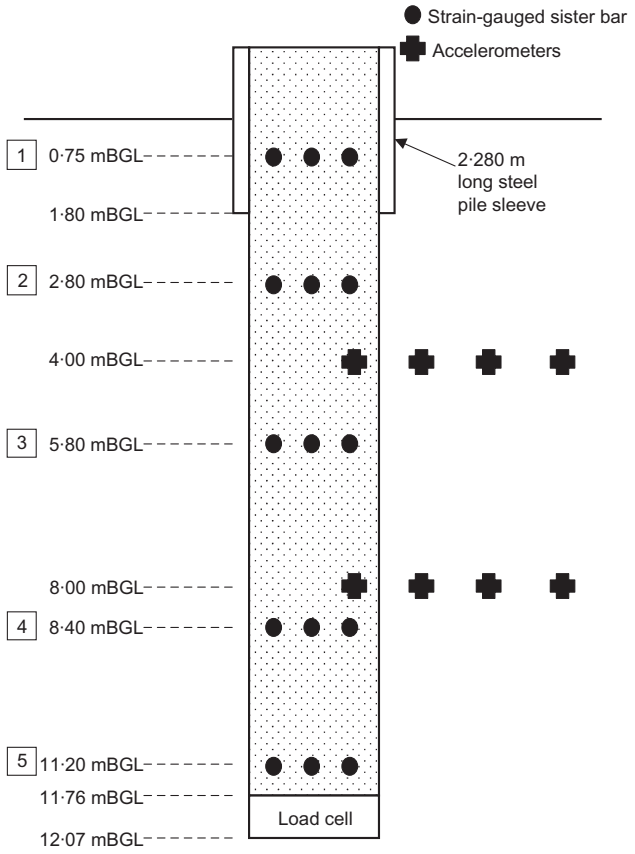

Fig. 4. Schematic of auger-bored pile and instrumentation locations (not to scale). Levels shown are initial levels prior to pile testing

Fig. 5. Pile-tip load cell with top plate removed and load columns visible

(Fig. 1). Load was measured by a load cell mounted in the base of the piston device. The pile settlement was measured by a photovoltaic sensor mounted in the base of the piston, which was excited by a laser reference beam (Middendorp, 2000). For static loading, reaction was provided by beams running over the test pile anchored to three auger-bored piles 11·5 m long and 600 mm in diameter arranged in a triangular pattern with two piles equidistant at 2·1 m from the test pile (centre to centre) and a third pile at the apex, 3·5 m distant. Load was applied to the test pile by a hydraulic jack and measured by an independent calibrated load cell. Pile settlement readings were provided by four linear variable

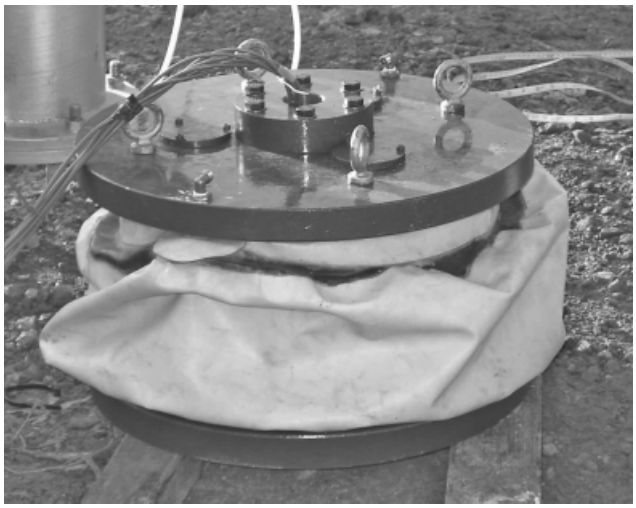

Fig. 6. Pile-tip load cell prior to installation with packer deflated

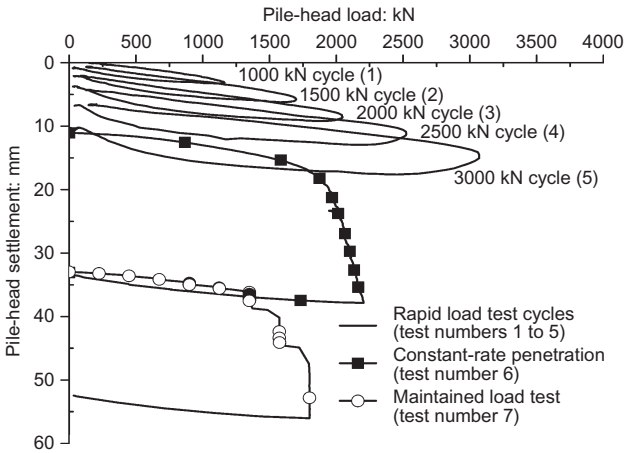

Fig. 7. Pile load–settlement history from different load-testing methods

displacement transducers (LVDTs) placed on the pile and referenced to a remote beam.

Load and settlement behaviour

The load–settlement behaviour for each of the pile tests is shown in Fig. 7. The loads measured during rapid load testing do not start at zero because, prior to testing, the 18 t reaction mass was lowered onto the pile. The settlement of the pile is not normally monitored during this operation. The settlements associated with the maximum pile-head loads are shown in Table 2. It is immediately apparent from comparison of the higher-magnitude rapid load tests (Tests 4 and 5) with the static tests (Tests 6 and 7) that, although much greater loads were applied to the pile during rapid load testing, the resulting maximum and residual deflections were smaller. Pile yield and ultimate resistance can be easily identified from the static test data. This is not so evident on inspection of the results from the rapid load tests despite the maximum load for the 3000 kN test exceeding the maximum static loads for CRP and MLT by factors of 1·39 and 1·71 respectively.

Load distribution on the pile during tests

To analyse the results from the embedded sister bars, it was necessary to determine the stiffness of the pile. The pile stiffness was determined in situ from the first loading cycle of the maintained load test by considering the strain in the uppermost sister bars (Level 1, Fig. 4) which were located within the sleeved section of the pile. The tangent modulus (E_{ct}) for concrete in the pile was calculated using (Delpak *et al.*, 1998)

$$E_{ct} = \frac{P_h - E_s A_{s1} \varepsilon_1}{\varepsilon_1 A_{c1}} \quad (1)$$

where P_h is the pile-head load (kN) applied in the first cycle, E_s is the Young's modulus of the steel (taken as 200 kN/mm^2), A_{s1} is the cross-sectional area of reinforcing steel in mm^2 at level 1 including the sleeve, ε_1 is the strain in the concrete at level 1, and A_{c1} is the cross-sectional area of the concrete pile at level 1.

The concrete tangent modulus was found to vary with increasing strain from 28 to 24 kN/mm^2. This compared with an average secant modulus of 31 kN/mm^2 found during concurrent laboratory testing of concrete cylinders (f_{cu} = 44 N/mm^2) to BS 1881 (BSI, 1983). Although Delpak *et al.* (1998) used a non-linear tangent modulus–strain relationship, a linear approach was found to be adequate in this case. This was then used to find the axial force (P_i) at the different levels in the pile using

$$P_i = \varepsilon_i \left[\left(-\frac{\mathrm{d}E_{ct}}{\mathrm{d}\varepsilon} \varepsilon_i + E_{ct0} \right) A_{ci} + E_s A_{si} \right] \quad (2)$$

where E_{ct0} is the apparent tangent modulus at zero strain.

The pile stiffness was calculated from the results of the MLT and used for the load transfer analyses for the CRP and rapid load tests.

The results from the load transfer analysis for the rapid load test with a target load of 3000 kN (Test 5) are shown compared with the CRP (Test 6) and MLT (Test 7) at various loads in Figs 8–10. The local unit shaft friction along with the calculated axial force along the pile was derived from the load gradients between the strain gauges. Values for the unit shaft resistance between strain gauge Levels 1 and 2 are not shown owing to the transition from the steel friction reducing casing to soil–concrete contact.

In Fig. 8 the loads are shown for the maximum load applied in each type of pile test (Table 2). In Fig. 9, comparison is made at a load of 1800 kN, which represents the

Table 2. Pile testing programme with pile load–settlement summary

Test no.	Test type	T_{su}: days	Target load: kN	Max. applied load: kN	δ_h at max load: mm	Max. δ_h during test: mm	δ_h at test end: mm	δ_h at test end/max. δ_h: %
1	RLT	35	1000	1163	3·13	3·27	0·88	27
2	RLT	35·7	1500	1700	5·08	5·50	1·46	27
3	RLT	35·7	2000	2048	6·46	7·09	1·68	24
4	RLT	35·7	2500	2525	6·86	8·63	2·48	29
5	RLT	35·8	3000	3071	7·92	10·96	4·42	40
6	CRP	56·9	–	2205	26·78	26·78	21·90	82
7	MLT	61·7	–	1800	23·05	23·05	19·47	85

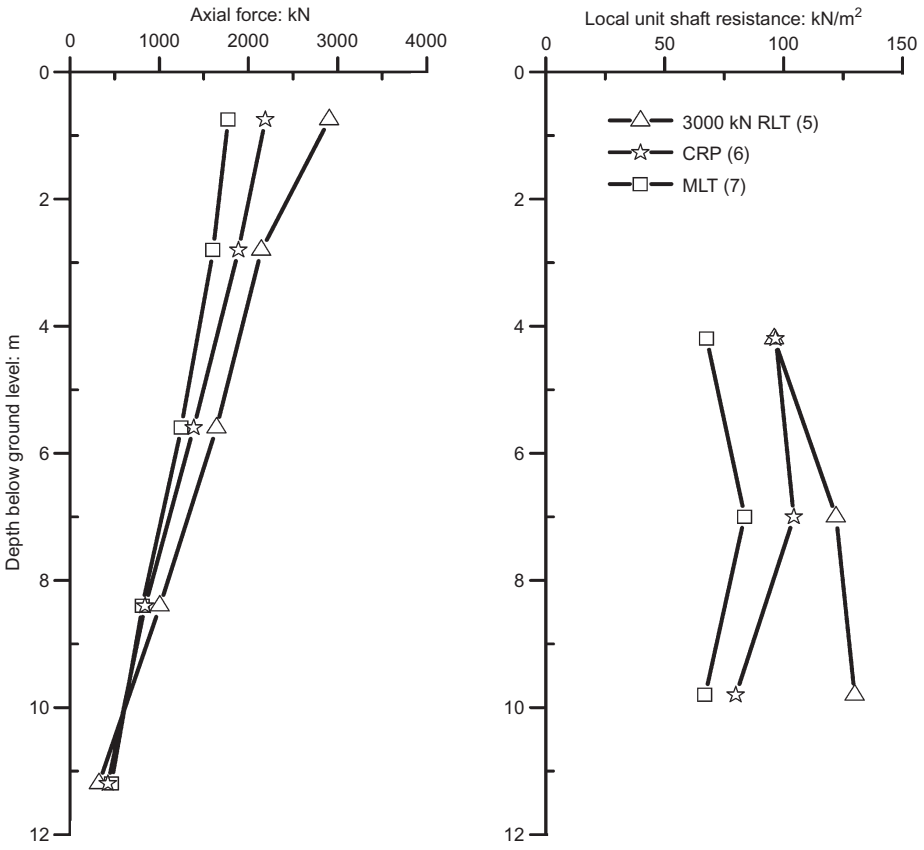

Fig. 8. Axial loads and shaft resistances from pile instrumentation during RLT and maintained load and constant rate of penetration static load tests at maximum applied loads

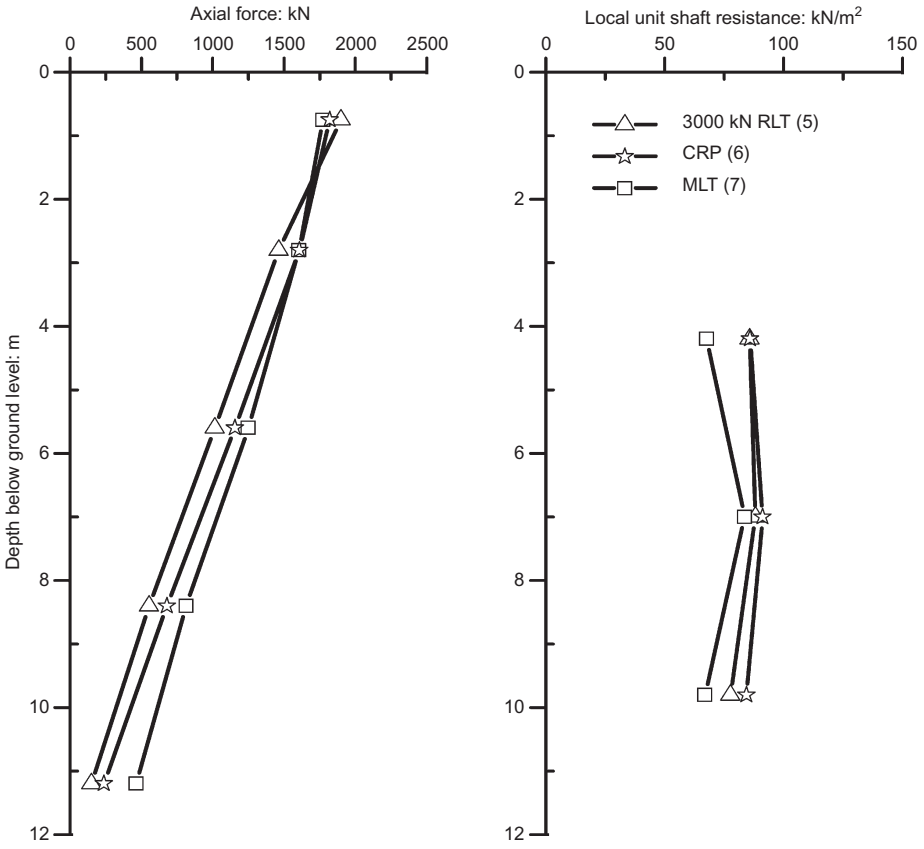

Fig. 9. Axial loads and shaft resistances from pile instrumentation during RLT and maintained load and constant rate of penetration static load tests (1800 kN load)

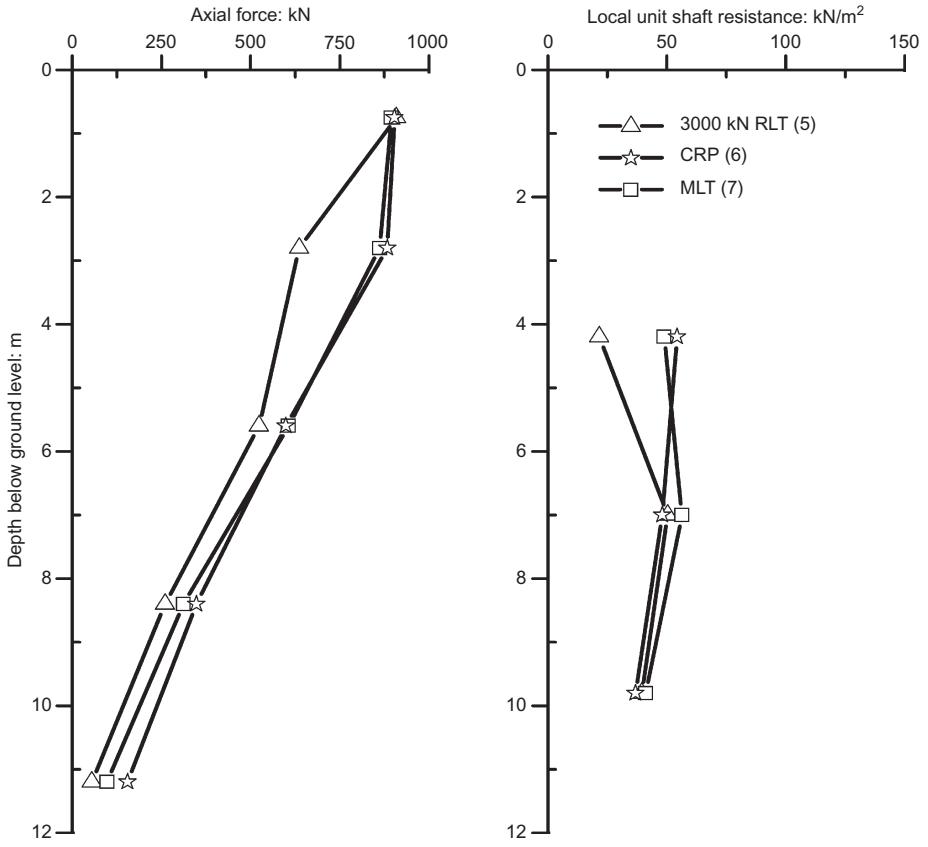

Fig. 10. Axial loads and shaft resistances from pile instrumentation during RLT and maintained load and constant rate of penetration static load tests (900 kN load)

maximum load applied during the ML test and corresponds to yield in the CRP test. In Fig. 10 the results are compared at a load of 900 kN, which corresponds to pre-yield conditions in each of the tests (Fig. 7).

Soil behaviour based upon acceleration measurements

The vertical accelerations were measured in the soil surrounding the pile during rapid load testing. Typical vertical accelerations measured in the pile and the surrounding soil can be seen in Figs 11 and 12 at 4 m BGL. The vertical ground accelerations follow the pile accelerations with diminished magnitude and a small phase shift. The changes in the ratio of soil to pile acceleration with radial distance from the pile at different load levels during the 3000 kN rapid load cycle are shown in Figs 13 and 14 for transducers located at 4 m and 8 m BGL respectively. The load levels at which the accelerations were compared were selected at significant peaks or features of the pile accelerations in Fig. 11, where similar points could be identified in each of the ground acceleration–time histories. This allowed ease of comparison between accelerometers and in effect eliminated the influence of phase lags.

The accelerations were integrated to determine the vertical displacements both in the soil and at the corresponding pile elevations. The average shear strains were then found by considering the relative vertical displacements between the accelerometers and their known separation. The shear strains are shown in Figs 15 and 16 at the mid-point between the

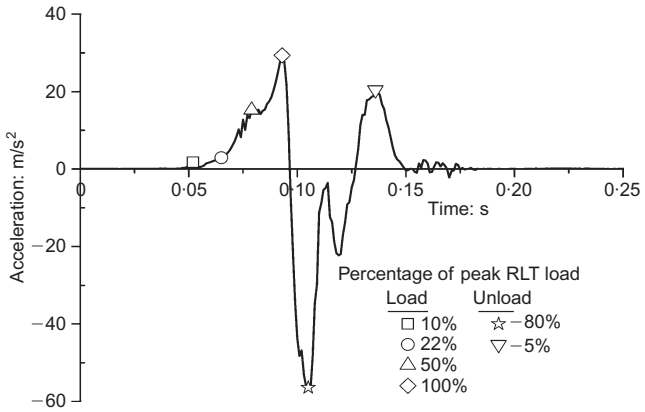

Fig. 11. Pile acceleration measured at 4 m BGL during 3000 kN RLT

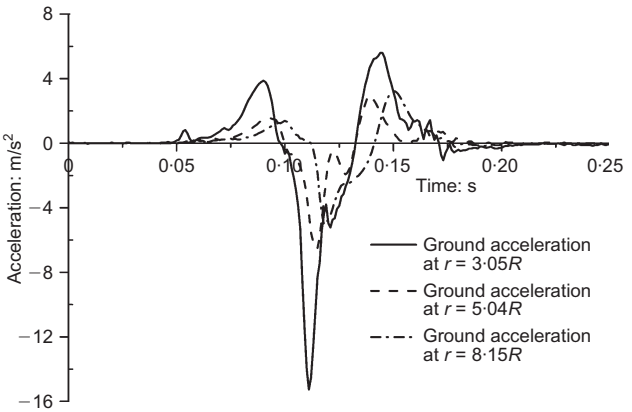

Fig. 12. Measured ground accelerations at 4 m BGL during 3000 kN RLT

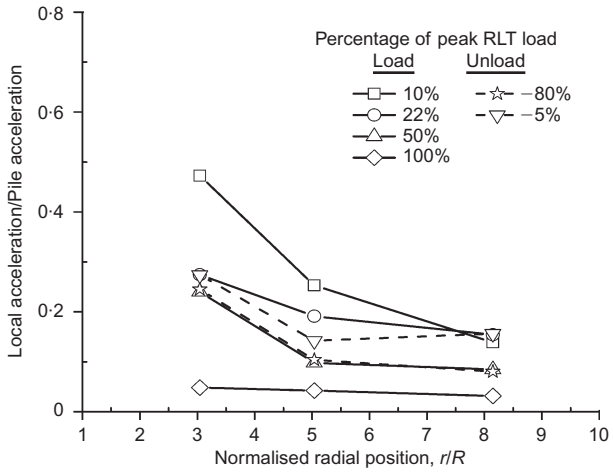

Fig. 13. Influence of pile loads on soil acceleration at 4 m BGL during 3000 kN RLT

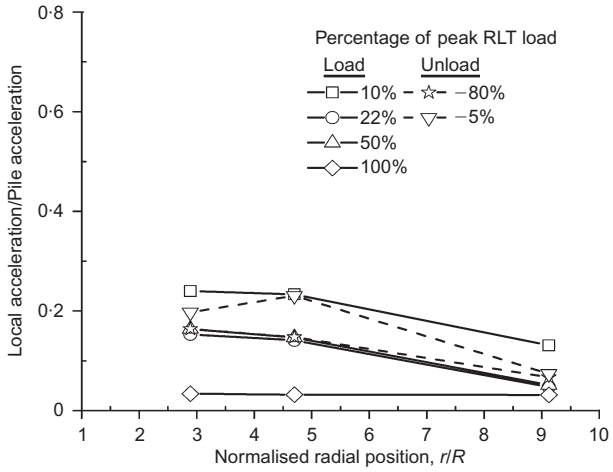

Fig. 14. Influence of pile loads on soil acceleration at 8 m BGL during 3000 kN RLT

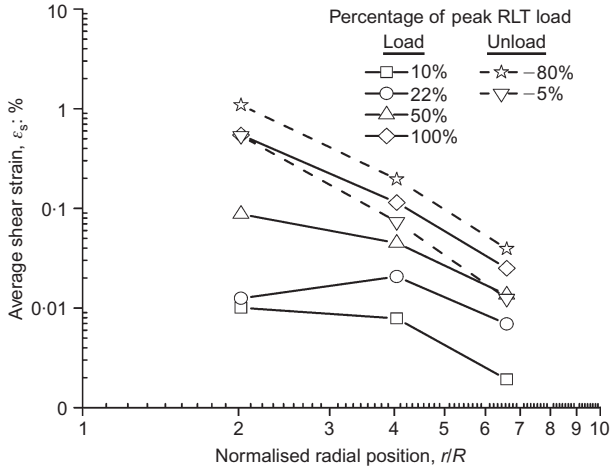

Fig. 15. Average shear strain at 4 m BGL during 3000 kN RLT

accelerometers. The engineering shear strains derived from the accelerometers were each considered at the same point in time. These strain values were then used to find indicative shear stresses (Figs 17 and 18) by using shear modulus values (G) for the appropriate strain level derived from monotonic triaxial testing and the in situ seismic CPT (Fig. 19).

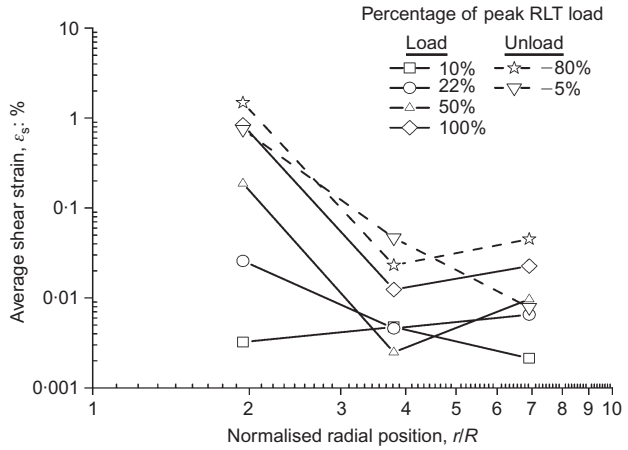

Fig. 16. Average shear strain at 8 m BGL during 3000 kN RLT

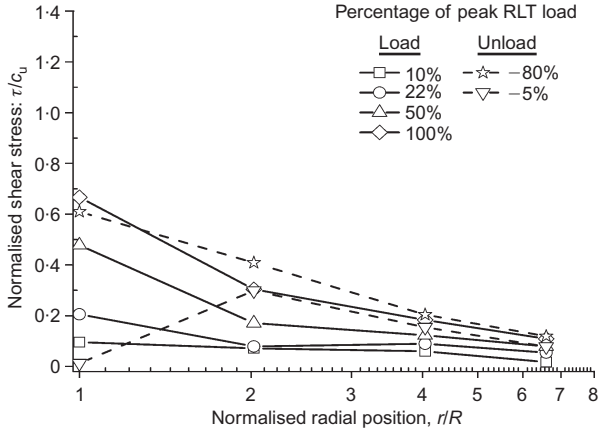

Fig. 17. Average shear stress at 4 m BGL during 3000 kN RLT

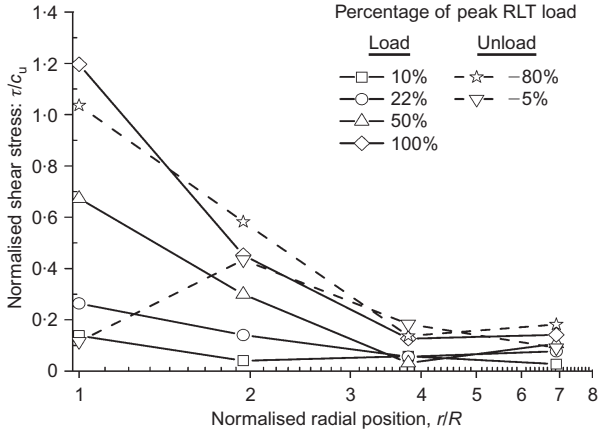

Fig. 18. Average shear stress at 8 m BGL during 3000 kN RLT

As the resolution of standard strain-measuring devices in triaxial testing is inadequate for determining strains over the range considered, comparison was made with previous determinations by Powell & Butcher (2003) and Hird *et al.* (1991). Their determinations were based upon a combination of laboratory and in situ techniques including resonant column tests, stress path triaxial testing with local strain measurement, self-boring and cone pressuremeters as well as large instrumented plate load tests. The shear modulus values derived from the monotonic triaxial tests on samples from 4 and 8 m BGL were normalised by the shear modulus

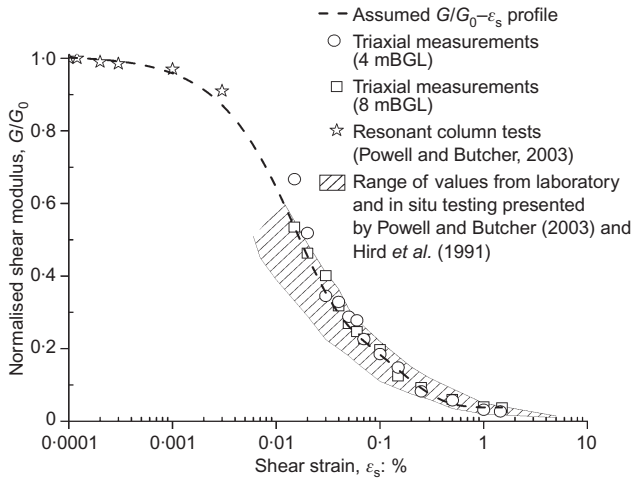

Fig. 19. Shear modulus profile used to determine average shear stresses from ground accelerometers

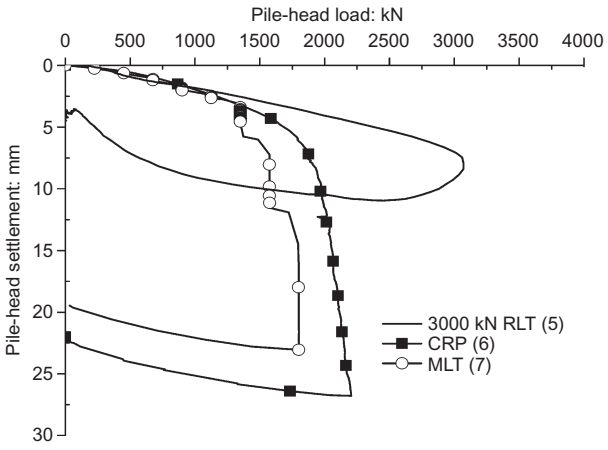

Fig. 20. Pile load–settlement history from different load testing methods (pile-head settlement zeroed)

determined from the seismic CPT results (G_0) at the appropriate depth, and show good correlation with those summarised from other studies. The best fit to the data from this study and those undertaken previously was then used to determine the appropriate shear modulus for the strains being considered. Values of shear stress at the pile interface were derived separately from the local unit shaft resistance based upon pile instrumentation readings, as shown in Figs 8–10.

DISCUSSION OF TEST PILE RESULTS

Instrumentation performance

Although the sister bar reinforcement and accelerometers performed without fault during the investigation, problems were experienced with the pile-tip load cell. These problems were characterised by non-uniform load distribution on the three columns in the load cell (Fig. 5) during the rapid load tests. Thus the pile-tip loads have not been presented, as they were not considered reliable. The skin friction might have been inferred below the lowest sister bar by assuming constant frictional resistance derived from the bars above, but this was avoided, as Borghi *et al.* (2001) showed that significant localised increase in elastic normal stresses may occur on the shaft near the tip due to end bearing. The non-uniform load on the pile-tip load cell may have been caused by tilting of the cell during installation.

Load and settlement behaviour

For the purposes of this paper the initial part of the load–displacement curve for each test will be referred to as the 'apparently linear' portion. The term 'elastic' has not been used to define this behaviour as the true elastic range of soil behaviour is much smaller than was measured during pile testing. The non-linear portion is then defined as the yielding or plastic zone. Comparison of the results from the different pile tests is shown in Fig. 20 with pile settlement reset to zero between tests. The load–settlement behaviour of the pile is very similar for all tests in the apparently linear zone up to 1000 kN, which is approximately 50% of the ultimate CRP static pile capacity. After this, the stiffness for the rapid load test exceeded the static load test stiffness as the static tests began to yield. The ML and CRP test had similar stiffness up to 1350 kN, at which point the MLT displayed an abrupt yield. Significant plunging of the pile during ML testing was encountered at a load of 1800 kN.

Although rapid load testing was taken to the maximum test load of 3000 kN, it can be assumed that larger residual pile settlements would have been achieved if greater loads had been applied. Based upon the results, it is proposed that the minimum applied target load during rapid load testing in clays must be at least 1·7 times the design ultimate static capacity to allow direct comparison of rapid and static tests.

Shaft capacity and load transfer

The load transfer from pile to soil was calculated from the change in pile load measured between two points. Examination of the change in axial force between the upper strain gauge positions (Levels 1 and 2) shown in Figs 8, 9 and 10 reveals that considerably greater load transfer occurred during rapid load testing than during the other types of test. This greater load transfer between Levels 1 and 2 for rapid load tests could be due to the upper very stiff clay layer, which had correspondingly high cone resistance and S-wave velocities, having a higher resistance to rapid loading despite the presence of the friction-reducing casing. Where axial loads are compared at similar load levels of 900 and 1800 kN for each test (Figs 9 and 10), loads in the pile shaft during rapid load testing are lower than those during static testing, thus indicating that greater load transfer had occurred at the top of the pile.

In Fig. 8 the maximum load levels are different in each case. However, the decay in axial force in the pile is greater for the rapid load test, indicating a higher degree of load transfer. This said, it is difficult to establish whether similar conditions of pile mobilisation had been reached in the rapid load test as in the static tests. Although far greater loads were applied during the rapid load test, much smaller residual deflections were observed (Table 2).

The peak shaft resistances shown in Fig. 8 illustrate the enhancement associated with rapid load tests at ultimate load conditions. The shaft resistance between 4 m and 10 m BGL for the rapid load test varied from 96 to 130 kN/m^2 at peak load, which is approximately 30% higher than the MLT results and 20% greater than the CRP values. At peak load during the rapid load test, the pile-head velocity was 475 mm/s compared with 0·01 mm/s during the CRP test. This confirms that pile shaft resistance is significantly influenced by pile loading rate after soil yielding has occurred. In contrast, the shaft resistances below Levels 1 and 2 for the rapid load test at load levels of 900 and 1800 kN are actually similar to or lower than those encountered in the static load tests even though the pile-head velocities were 70 and 290 mm/s respectively. At these load levels (900 and

1800 kN) the 3000 kN rapid load test result was still in the pre-yield apparently linear phase rather than the post-yield plastic phase of loading (Fig. 20), and much of the load transfer was occurring in the stiff near-surface clay layer. When the rapid load test results are compared with the static results in the pre-yield apparently linear phase of the test there is no significant enhancement of stiffness. This implies that the rate-dependent or viscous behaviour was not initiated until yield of the soil had occurred (Fig. 20). This is consistent with laboratory element testing of fine-grained soils presented by Tatsuoka *et al.* (1997), who showed that there was no rate effect within the elastic region of a soil's behaviour at very small strains. As the strain level increased towards that consistent with the apparently linear phase of pile behaviour the soils displayed a high degree of rate sensitivity. Richardson & Whitman (1963) and Lefebvre & LeBoeuf (1987) also noted that pore pressure was unaffected by strain rate at strains less than 0·5%, although it should be noted that the maximum strain rates used in these laboratory studies are typically closer to those associated with static pile tests.

Soil behaviour derived from ground accelerations

The ground accelerations had decayed markedly by a radial distance $3R$ and had fallen below 20% of the pile's acceleration by $6R$. It is clear from Figs 13 and 14 that the ground accelerations vary with changing load level during a rapid load test. These accelerations are at a maximum at low loads, reducing to a minimum at peak load. This would suggest a decoupling of the pile acceleration from that of the soil on approaching peak load, as originally proposed by Randolph & Simons (1986), who suggested that acceleration of the soil mass would occur only during the initial pre-yield apparently linear loading phase. After this, the pile and a relatively small annulus of soil would shear relative to the larger soil mass, and rate-dependent soil shear resistance would need to be considered. This model of pile–soil load transfer is consistent with the measurements of shaft resistance discussed above, where little enhancement of shaft resistance was noted prior to yielding. This said, the soil again begins to accelerate with the pile during unloading. For instance, in Fig. 13 during unloading the proportion of acceleration experienced by the soil (local acceleration) at 80% peak RLT load is similar to that observed at 50% peak RLT load during the loading phase.

The derived shear strains (Figs 15 and 16) show increasing average shear strain in the soil with increasing applied pile load up to peak load. After this the shear strain continues to increase as the pile unloads. This is consistent with the typical RLT load–displacement behaviour shown in Fig. 20, where maximum pile displacement occurs at post-peak loads. The strains at 4 m and 8 m BGL (Figs 15 and 16) are similar in magnitude, but at 8 m BGL the smooth radial decay of strains is not apparent between $3R$ and $4R$. This is due to the adjacent accelerometer readings having comparable magnitudes between $2{\cdot}89R$ and $4{\cdot}70R$ (Fig. 12), which may have been the result of a variation in localised radial soil properties or the presence of a stiff inclusion. The results show that the shear strains at $2R$ and beyond may be classified as small strain (as defined by Viggiani & Atkinson, 1995) during the RLT test, with large strains being experienced only at $2R$ at maximum pile displacement and beyond.

The radial variation of average vertical shear stress normalised by the undrained shear strength is shown in Figs 17 and 18. The shear stresses are consistent with the strains, except that the stresses at the pile/soil interface obtained from the pile instrumentation are a maximum at the peak applied pile load. During unloading the shaft resistance reduces rapidly, resulting in a lag between the change in soil stress close to the pile and that at a distance such that when the load has reduced to 5% of the peak value the shear stress at $2R$ is higher than the shaft friction.

In Figs 13 and 14 the acceleration ratios from $4{\cdot}5R$ outwards were similar for the two levels of 4 m and 8 m; the proportion of acceleration at $3{\cdot}05R$ at 4 m BGL was greater for all but the peak load. This is likely to have been influenced by the degree of mobilisation of soil shear strength, which, as can be seen in Figs 17 and 18, was significantly lower at 4 m BGL than at 8 m BGL.

ANALYSIS OF RAPID LOAD TESTS IN GLACIAL TILL

The aim of undertaking rapid load testing was to obtain the equivalent ultimate static pile behaviour and to test the findings as part of a Class B prediction (Lambe, 1973). Randolph & Deeks (1992) proposed that the ultimate shaft resistance of a pile subjected to loading at elevated penetration rates during dynamic testing could be represented by

$$\tau_d = \tau_s \left[1 + \alpha \left(\frac{\Delta v}{v_0} \right)^{\beta} - \alpha \left(\frac{\Delta v_{min}}{v_0} \right)^{\beta} \right] \tag{3}$$

where τ_d is the pile shaft resistance at an elevated penetration rate; τ_s is the shaft resistance at a low penetration rate, similar to those encountered during static pile testing; Δv is the relative pile/soil slip velocity; Δv_{min} is the relative pile/soil slip velocity in a 'static' test; v_0 is a reference velocity taken as 1 m/s; and α and β are rate parameters. The equation above is based upon that proposed by Smith (1962) for dynamic soil pile interaction but modified to incorporate non-linear rate effects, as proposed by Gibson & Coyle (1968).

Simulation of model rapid load tests by Brown *et al.* (2004) verified that equation (3) was also valid for the rates of penetration associated with rapid load testing, which are lower than those encountered during dynamic testing. Brown (2004) proposed that, for determination of the ultimate static equivalent pile resistance from a rapid load test in fine-grained soils ($F_{static(ultimate)}$), where the majority of a pile's capacity was derived from shaft resistance, the following could be used.

$$F_{static(ultimate)} = \frac{F_{STN} - (M\ddot{x})_{Pile}}{1 + \alpha(\Delta v/v_0)^{\beta} - \alpha(\Delta v_{min}/v_0)^{\beta}} \tag{4}$$

where F_{STN} is the measured pile-head load, M is the mass of the pile, and $\ddot{x}$ is the measured or calculated pile acceleration.

Values for the parameters $\alpha = 1{\cdot}26$ and $\beta = 0{\cdot}34$ were obtained by Brown (2004) testing model piles in a calibration chamber in a kaolin, silt and sand mixture. The model piles instrumented with pore water pressure and skin and tip load transducers were made from stainless steel with a diameter of 70 mm and a typical embedded length of 800 mm. They were installed in pre-bored holes prior to final consolidation, and CRP testing was undertaken at rates up to 500 mm/s. Balderas-Meca (2004), testing both the calibration chamber clay and the glacial till described above using varying-rate triaxial shear tests, showed that the rate parameters, though different under triaxial conditions, were almost identical for the two materials. The calibration chamber values were therefore adopted for analysing the full-scale pile test data.

The results of this method of analysis for the 3000 kN rapid load test are presented in Fig. 21. These results have been compared with those obtained by using the unloading point method (Kusakabe & Matsumoto, 1995). The pile-head settlement chosen as the point of comparison for the three

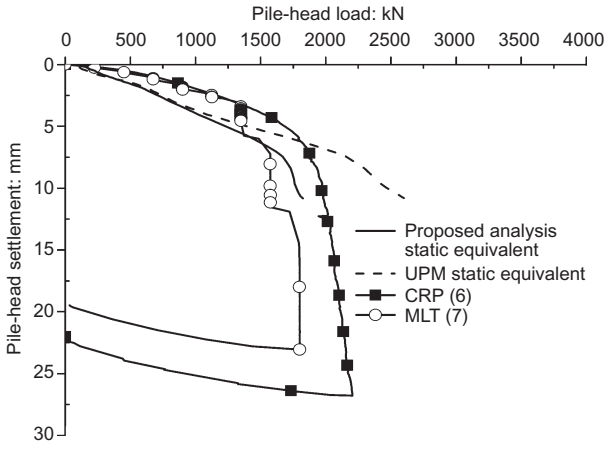

Fig. 21. Comparison of derived ultimate static equivalent pile behaviour with measured static CRP and ML tests

types of test was limited by the deflection in the rapid load test. A deflection of 8·85 mm was chosen because this was a recorded data point close to the peak for the rapid load test and within the ultimate yield zones for the ML and CRP test. The predicted static capacity of 1746 kN was only 10% less than the measured CRP load of 1946 kN. In comparison, the unloading point method (UPM) overpredicts the pile capacity by 31% and fails to define a clear yield point. Although the rate parameters used in equation (4) were based upon model pile CRP tests (Brown, 2004), it is interesting to compare the results with the MLT data, particularly as the maintained load test is the preferred method of testing piles in the UK. The maximum predicted load of 1746 kN compares well with the load of 1800 kN at which plunging of the pile occurred during MLT.

Application of the analysis in the pre-yield phase of loading results in an underprediction of stiffness. This is also true for the UPM. This is not surprising, as the empirical rate parameters used in equation (4) were developed based upon ultimate model pile behaviour as discussed above. Results from soil accelerometers suggest that the soil surrounding the shaft has limited inertial and damping resistance during this phase of loading. It is interesting to note that static and raw RLT load–settlement data up to 30% of the peak rapid load are very similar and may offer an empirical method of estimating pile stiffness up to working loads (Fig. 20).

It should be noted that the results from the analysis of the rapid load test and the subsequent comparison with the results of static pile testing will be affected by the adoption of multiple testing of a single pile. This approach is likely to have greatest influence on the results from the pre-yield phase of loading. This can be seen in the work of Marsland & Powell (1980), who, carrying out a series of large-diameter cyclic plate load tests in the same till deposit, showed that there was no significant change in ultimate capacity measured by CRP testing after cyclic loading, but there was an overall stiffening of response in the pre-yield phase. Lehane & Jardine (1994), testing model jacked-in displacement piles at the same site, concluded that retesting the piles resulted in alteration of the soil fabric, described as plastic hardening, with radial effective stresses being approximately 15% higher in all retests. However, the relative disturbance of the soil fabric is likely to be greater for a displacement pile than for the auger-bored pile described here.

The results of this study highlight the need for an appreciation of the significance of damping in clay soils when specifying rapid load pile testing. To develop a full RLT analysis method greater knowledge is required of soil rate effects for different soil types. These parameters may be derived from full-scale RLT-static comparisons or laboratory model and element tests, as undertaken by Brown (2004) and Balderas-Meca (2004).

CONCLUSIONS

Rapid load pile tests offer the potential for cost and time savings for the quality control of deep foundations. Load transfer data obtained from a full-scale instrumented pile in a glacial clay, which derived the majority of its capacity from skin resistance, have been used to show that enhanced shaft resistance as a result of viscous rate effects is significant only after yield of the pile–soil interface. Prior to this, in the apparently linear phase of loading there was no significant enhancement of shaft resistance due to penetration rate.

Accelerometers in the pile and surrounding soil indicated that the proportion of acceleration transferred to the ground reduced with increasing pile load up to the peak rapid load. The low soil accelerations at the peak rapid load provided evidence of decoupling of the pile acceleration from the surrounding ground. Vertical shear strains derived from the acceleration readings were in all cases reduced to less than 1% beyond two pile radii.

A simple non-linear viscous rate model originally proposed by Randolph & Deeks (1992) gave a Class B prediction of ultimate pile capacity that lay between the values obtained for static ML and CRP tests. Use of this model in the apparently linear zone significantly underestimated pre-yield pile stiffness. It is, however, interesting to note that static and raw RLT load displacement data up to 30% of the peak rapid load are very similar, and this may offer an empirical method of estimating pile stiffness up to working loads, although this point requires verification for a pile that has only been subjected to first time static loading.

Where rapid load pile testing is specified in clay soils, care should be taken to verify that the testing device has sufficient capability to mobilise the test pile capacity at elevated pile penetration rates. To allow derivation of the equivalent ultimate static pile behaviour from rapid load tests in clays, the minimum applied target load must be at least 1·7 times the predicted ultimate static capacity.

ACKNOWLEDGEMENTS

This research project was funded by the Engineering and Physical Sciences Research Council (Grant No. GR/R46939/01). Technical assistance was provided by Berminghammer Foundation Equipment (Canada) and TNO Building Research (Netherlands). The Expanded Piling Company (UK) kindly installed the piles and provided the research site facility. Rapid load testing and static pile load testing were undertaken by Precision Monitoring and Control (UK). Cone penetration testing and ground accelerometer installation were undertaken by Lankelma. Thanks are also extended to Dr Juan Balderas-Meca for provision of the results from element testing of the glacial lodgement till.

NOTATION

A_{ci}	cross-sectional area of concrete at pile level i
A_{si}	cross-sectional area of steel at pile level i
C_c	slope of normal compression line
c_u	undrained shear strength
E_{ct}	tangent modulus of concrete
e_0	voids ratio of normally consolidated soil at $p' = 1{\cdot}0$ kPa
E_s	Young's modulus of steel
$F_{static(ultimate)}$	derived equivalent ultimate static pile resistance

F_{STN} measured rapid load test pile resistance
f_{cu} concrete cube strength
f_s sleeve friction
G shear modulus
G_o shear modulus from seismic wave measurements
M mass of element under consideration
N standard penetration test N value
P_h pile-head load
P_i pile axial force at level i
q_c cone resistance
R pile radius
r radial position under consideration
T_{su} time interval between pile installation and pile testing
Δv relative velocity of pile and soil
v_0 reference velocity
v_{min} lowest velocity used in derivation of rate parameters
$\ddot{x}$ pile acceleration
α damping constant
β damping constant
δ_h pile-head settlement
ε_s shear strain
ε_i strain in the concrete at pile level i
τ shear stress
τ_d shaft resistance at elevated rates
τ_s shaft resistance at low rates

REFERENCES

Anderson, W. F. (1974). The use of multistage triaxial tests to find the undrained strength parameters of stony boulder clay. *Proc. Inst. Civ. Engrs* **57**, Part 2, 367–372.

Balderas-Meca, J. (2004). *Rate effects in rapid loading of clay soils*. PhD thesis, University of Sheffield, UK.

Bell, A. (2001). *Investigation into the increase in capacity with time of precast piles driven into stiff overconsolidated clay.* MSc thesis, University of Sheffield, UK.

Berridge, N. G. & Pattison, J. (1994). *Geology of the Country Around Grimsby and Partington — Memoir for 1:50 000 Geological Sheets 81 & 82 and 90 & 91.* Nottingham: British Geological Survey.

Borghi, X., White, D. J., Bolton, M. D. & Springman, S. (2001). Empirical pile design based on cone penetrometer data: an explanation for the reduction of unit base resistance between CPTs and piles. *Proc. 5th Int. Conf. on Deep Foundations Practice, Singapore*, 125–132.

British Standards Institution (1983). *Testing concrete: Method for determination of static modulus of elasticity in compression*, BS 1881:Part 121. Milton Keynes: BSI.

Brown, D. A. (1994). Evaluation of static capacity of deep foundations from Statnamic testing. *Geotech. Test. J. ASTM* **17**, No. 4, 403–414.

Brown, M. J. (2004). *The rapid load testing of piles in fine grained soils*. PhD thesis, University of Sheffield, UK.

Brown, M. J., Anderson, W. F. & Hyde, A. F. L. (2004). Statnamic testing of model piles in a clay calibration chamber. *Int. J. Phys. Modelling Geotech.* **4**, No. 1, 11–24.

Delpak, R., Robinson, R. B. & Omer, J. R. (1998). Assessment of the performance of large-diameter bored cast in situ piles formed in Mercia Mudstone. *Proceedings of the CIRIA conference on the engineering properties of the Mercia Mudstone Group,* Derby, pp. 36–63.

Dunnicliff, J. & Green, G. E. (1988). *Geotechnical instrumentation for measuring field performance*. New York: Wiley.

Gibson, G. C. & Coyle, H. M. (1968). *Soil damping constants related to common soil properties in sands and clays (bearing capacity for axially loaded piles)*, Research Report 125-1, Study 2-5-67-125, Texas A&M University, Texas, Texas Transportation Institute.

Hird, C. C., Powell, J. J. M. & Yung, P. C. Y. (1991) Investigation of the stiffness of a glacial clay till. *Proc. 10th Eur. Conf. Soil Mech. Found. Engng, Florence*, 107–110.

Holeyman, A. E., Maertens, J., Huybrechts, N. & Legrand, C. (2000). Results of an international pile dynamic testing prediction event. *Proc. 6th Int. Conf. on the Application of Stress Wave Theory to Piles, Sao Paulo*, 725–732.

Hyde, A. F. L., Robinson, S. A. & Anderson, W. F. (2000). Rate effects in clay soils and their relevance to Statnamic pile testing. *Proc. 2nd Int. Statnamic Seminar, Tokyo*, 303–309.

Institution of Civil Engineers. (1997). *Specification for piling and embedded retaining walls*, 1st edn. London: Thomas Telford.

Kusakabe, O. & Matsumoto, T. (1995). Statnamic tests of Shonan test program with review of signal interpretation. *Proc. 1st Int. Statnamic Seminar, Vancouver*, 113–122.

Lambe, T. W. (1973) Predictions in soil engineering. *Géotechnique* **23**, No. 2, 149–202.

Lefebvre, G. & Leboeuf, D. (1987). Rate effects and cyclic loading of sensitive clays. *J. Geotech. Engng ASCE* **113**, No. 3, 476–489.

Lehane, B. M. & Jardine, R. J. (1994) Displacement pile behaviour in glacial clay. *Can. Geotech. J.* **31**, No. 1, 79–90.

Marsland, A. & Powell, J. J. M. (1980) Cyclic load tests on 865 mm diameter plates in a stiff clay till. *Proceedings of the international symposium on soils under cyclic and transient loading, Swansea*, pp. 837–847.

McVay, M. C., Kuo, C. L. & Guisinger, A. L. (2003) *Calibrating resistance factor in the load and resistance factor design of Statnamic load testing*, Research Report 4910–4504–823–12, Contract BC354, RPWO#42. University of Florida, Florida Department of Transportation.

Middendorp, P. (1993). First experiences with Statnamic load testing of foundation piles in Europe. *Proc. 2nd Int. Geotech. Seminar on Deep Foundations on Bored and Auger Piles, Ghent*, 265–272.

Middendorp, P. (2000). Statnamic the engineering of art. *Proc. 6th Int. Conf. on the Application of Stress Wave Theory to Piles, Sao Paulo*, 551–561.

Middendorp, P. & Bielefeld, M. W (1995). Statnamic load testing and the influence of stress wave phenomena. *Proc. 1st Int. Statnamic Seminar, Vancouver*, 207–220.

Mullins, G., Lewis, C. L. & Justason, M. D (2002). Advancements in Statnamic data regression techniques. *Proceedings of the ASTM International Deep Foundations Congress*, ASTM Geotechnical Special Publication No. 116, Vol. 2, pp. 915–930. West Conshohocken, PA: ASTM International.

Nishimura, S. & Matsumoto, T. (1995). Wave propagation analysis during Statnamic loading of a steel pipe. *Proc. of 1st Int. Statnamic Seminar, Vancouver*, 23–33.

Powell, J. J. M. & Butcher, A. P. (2003) Characterisation of a glacial till at Cowden, Humberside. *Proceedings of the international conference on the characterisation and engineering properties of natural soils*, Singapore, pp. 983–1019.

Randolph, M. F. & Deeks, A. J. (1992). Dynamic and static soil models for axial response. *Proc. 4th Int. Conf. on the Application of Stress Wave Theory to Piles, The Hague*, 3–14.

Randolph, M. F. & Simons, H. A. (1986). An improved soil model for one-dimensional pile driving analysis. *Proc. 3rd Int. Conf. on Numerical Methods in Offshore Piling, Nantes*, 3–17.

Richardson, A. M. & Whitman, R. V. (1963). Effect of strain rate upon undrained shear resistance of a saturated remoulded fat clay. *Géotechnique* **13**, No. 4, 310–324.

Smith, E. A. L. (1962). Pile-driving analysis by the wave equation. *J. Soil Mech. Found. Div. ASCE* **127**, Part I, 1145–1193.

Tatsuoka, F., Jardine, R. J., Lo Presti, D., Di Benedetto, H. & Kodaka, T. (1997). Characterising the pre-failure deformation properties of geomaterials. *Proc. 14th Int. Conf. Soil Mech. Found. Engng, Hamburg*, 2129–2164.

Taylor, P. T. (1966). *Age effects on shaft resistance and effect of loading rate on load distribution of bored piles*. PhD thesis, University of Sheffield, UK.

Viggiani, G. & Atkinson, J. H. (1995). Stiffness of fine-grained soil at very small strains. *Géotechnique* **45**, No. 2, 249–265.

Weltman, A. J. & Healy, P. R. (1978). *Piling in Boulder Clay and other glacial tills*, CIRIA Report No. PG5. London: DOE and CIRIA Piling Group.

Wood, T. (2003). *An investigation into the validation of pile performance using Statnamic tests*. MSc thesis, Imperial College of Science, Technology and Medicine, UK.